

COMPARISON OF FRACTURE CHARACTERISTICS OF OPEN-HOLE-NOTCH CARBON-FIBER-REINFORCED COMPOSITES SUBJECTED TO TENSILE AND COMPRESSIVE LOADINGS

M.-U. Saeed,* Z. F. Chen, Z. H. Chen, and B. B. Li

Keywords: scanning electron microscopy (SEM), open-hole tension (OHT), open-hole compression (OHC), fiber pull-out, microbuckling

Open-hole tension (OHT) and open-hole compression (OHC) tests were carried out on hot-pressed carbon-fiber-reinforced composite samples with a singular open hole. The fracture surfaces of the OHT- and OHC-tested specimens were examined by using scanning electron microscopy (SEM). SEM micrographs showed significant features on the surface of carbon fiber, matrix, and especially in the fiber/ matrix interface. Interpretation of these micrographs revealed the possible failure mechanism of composite samples with an open hole under tensile and compressive loadings. Furthermore, a comparative study of these micrographs also pointed to certain specific differences between the fracture characteristics of open-hole composite samples failed under tension and compression. This information is useful in the post-failure analysis of a composite structure.

1. Introduction

Holes are drilled in carbon-fiber-reinforced composite structures to accommodate bolts and rivets in order to join two or more composite parts or subassemblies. However, these holes cause a large decrease in the strength and alter the failure mechanisms of composites. This decrease in strength and change in the damage mechanism depends upon various geometrical and material parameters, such as the lay-up sequence, hole size, ply and laminate thicknesses, specimen width, fiber volume fraction, strain rate, and the size and role of delamination [1-12]. Many researchers have implemented (i)

College of Material Science and Technology, Nanjing University of Aeronautics and Astronautics, 29#, Yudao Road, Nanjing 210016, PR China

*Corresponding author; tel.: +862552112909; e-mail: zhaofeng_chen@163.com, umar_engg@yahoo.com

Russian translation published in *Mekhanika Kompozitnykh Materialov*, Vol. 52, No. 6, pp. 1069-1080, November-December, 2016. Original article submitted November 21, 2014; revision submitted April 26, 2016.

fracture mechanics, (ii) characteristic distance, and (iii) progressive damage approaches to estimate such effects due to the presence of open holes [13-20]. Each approach has its own advantages and disadvantages, and they all are complimentary to each other.

In addition to theoretical and numerical studies on the open-hole strength, numerous attempts have been made to elucidate the damage mechanisms of composite laminates with open holes under tensile and compressive loading by using different characterizing techniques, such as the Electronic Speckle Pattern Interferometry (ESPI) and full-field displacement measurements used by Farge et al. [21] to characterize the damage of cross-ply carbon fiber/ epoxy laminates. Their results suggest that the damage is initiated at the crack scale and the change in crack density can be considered as the major cause for their stiffness reduction. Pierron et al. assessed the damage mechanisms of open-hole composite specimens by using full-field strain measurements [19, 20]. It was clearly shown that, before the onset of surface cracking, a significant subsurface cracking occurred at the hole in the 90° plies, which later propagated away from the hole. Yudhanto et al. examined the damage growth in open-hole carbon/epoxy laminates in tension by using microscopy [22-24]. Their observations revealed that the stress concentration around the hole caused the failure of open-hole specimens. Suemasu et al. studied the failure mechanism of quasi-isotropic composite laminates with an open hole under compression by using ultrasonic C-scans [13]. They showed that the microbuckling of fibers in the 0° layers appeared first and was followed by their further microbuckling and interlaminar delaminations in several interfaces before the final unstable failure. Lee et al. employed X-ray radiography and C-scanning to study the failure behavior of open-hole composite laminates in compression [7]. They showed that the specimens failed from the hole in a direction almost perpendicular to the loading direction and the damage initiated and grew in the form of matrix cracking, delamination, and fiber microbuckling. O'Higgins et al. compared the open-hole tension characteristics of high-strength glass- and carbon-fiber-reinforced composite materials [25]. They reported that the progression of damage in the two materials pointed to a very similar damage and failure sequence, which consisted of matrix cracking in the ±45° and 90° plies, followed by extensive delamination prior to failure. This work was focused on the characterization of damage mechanisms of the open-hole tensile and compressive failure, paying less attention to the failure characteristics in OHT and OHC, by using fractography techniques, the SEM in particular. Fractographic analyses (using the SEM) of fracture surfaces of failed structural components revealed useful information about the cause and sequence of failure. These surfaces revealed features concerning the origination of cracks, their propagation direction, the failure mode, load, and environmental conditions at the instant of failure. This knowledge is very effective in revealing the cause of failure. Hence, a similar need arose to understand the fractographic evidence which open-hole composite materials can provide under tensile and compressive loadings. The aim of this research was to identify the key fracture surface characteristics for hole-notched carbon-fiber-reinforced composites subjected to tensile and compressive loadings.

2. Experimental

2.1. Materials and manufacture of composites

The carbon-fiber-reinforced composites were manufactured by the method of hot pressing using a CF3052 twill-weave carbon fabric and a 3238A epoxy resin. Two composite sheets were prepared — one for OHT and the other for OHC tests. Ten layers of the carbon fabric were used to produce a 2.4-mm-thick sheet and 15 layers 3.6 mm thick for OHT and OHC tests, respectively. The resin was applied to the carbon fabric layers by hand lay-up cured in a hot press at a 125°C temperature and 0.5 MPa pressure for 4 h. The composite sheets were then demolded and cut into 300 × 36-mm samples. A 6-mm hole was drilled in each sample at its center as per ASTM standards D5766 [26] and D6484 [27] for OHT and OHC tests, respectively.

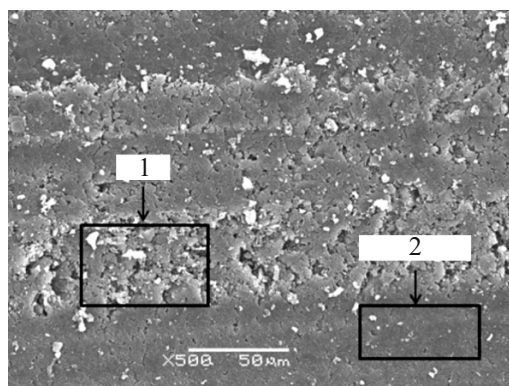


Fig. 1. Photomicrograph of the surface of a hole created by drilling: 1 — resin and 2 — carbon fiber.

2.2. OHT and OHC tests

The OHT and OHC tests were performed according to ASTM standards D5766 and D6484 on at least five samples. All the tests were carried out in a CMT 5105 testing machine at a crosshead speed of 1.25mm/min up to failure. The load–displacement data were recorded by an automated software attached to the mechanical testing machine.

2.3. Characterization of fracture surface

The fracture surfaces from the OHT and OHC tests were studied by a JEOL-JSM 6360LV scanning electron microscope to identify fracture differences between the OHT and OHC tests and their associated failure mechanisms.

3. Results and Discussion

3.1. OHT and OHC strengths

The mean ultimate OHT strength of composite samples was found to be 326.6 MPa. The SD and CV (%) of OHT samples were 10.53 and 3.23, respectively. The mean ultimate OHC strength of the composite samples was 270.3 MPa. The SD and CV (%) of the OHC samples were 6.97 and 2.58, respectively.

3.2. Comparison of fracture characteristics

The fracture surface obtained after the failure of a composite sample under tensile, compressive, or shear loading possess certain macro- and microscopic characteristic fracture markings that enables one to evaluate and study the fracture process. These markings usually emerge on the fiber surface, resin matrix, and, most importantly, on the fiber/ matrix interface. The markings that appear on the surface of fibers parallel, perpendicular, or at some angle to the loading direction are significantly different from one another and provide useful information about the fracture mechanism. Upon application of a tensile or compressive load to an open-hole composite sample, fracture started by breakage of the weakest fibers, just beside the open-hole.

Figure 1 presents a photomicrograph of the inner surface of a hole created by drilling in a composite sample. Several microcracks were identified both in the matrix and fiber phases, which were more prominent in the matrix. They were produced by the stresses generated by drilling. These stresses caused greater damage, in the form of micro- and macrocracks, to the resin

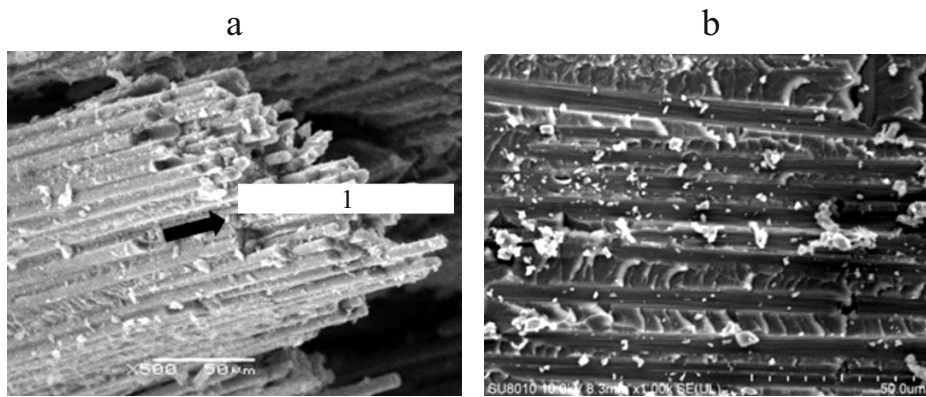


Fig. 2. River marks in the resin among fibers, showing the direction of crack growth (1) in OHT (a) and OHC (b) samples.

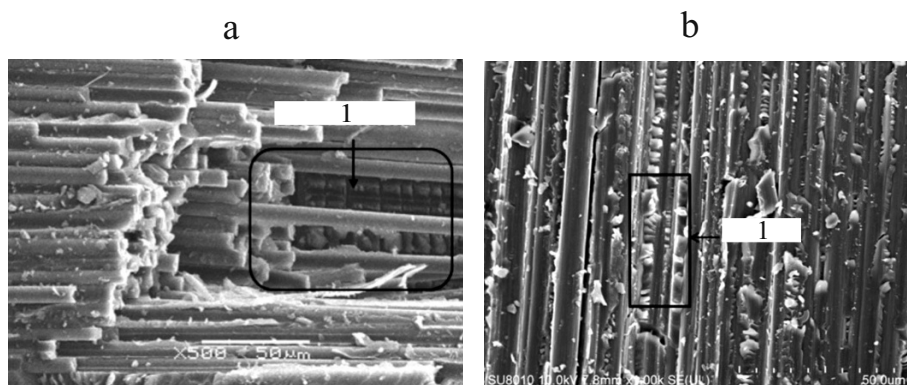


Fig. 3. Shear marks (1) in the resin in OHT (a) and OHC (b) samples.

than fibers. Upon application of a tensile or compressive load, the numerous microcracks coalesced and formed a visible crack. In the OHT samples, the crack seemed to generate from the center (the open-hole area) and propagated towards their edges perpendicular to the applied tensile load. In the OHC samples, the crack also initiated from the open hole, but grew along the center line in a random direction (not necessarily from the center towards the edge).

In the resin adhered to the fiber surface in the OHT samples, river marks could be seen, as illustrated in Fig. 2a, which pointed to the presence of interlaminar shearing. These marks were formed by the coalescence of numerous small 45° tensile microcracks in the resin between fibers. The size, shape, and morphology of these marks varied over the fracture surface depending on the amount of resin between fibers, fiber orientation, and the percentage of shear. Direction of these marks showed the overall growth direction of crack, which seemed to start from the open hole towards sample edges.

Similar river marks generated by interlaminar shearing between carbon fibers in an OHC sample are shown in Fig. 2b, which are more prominent than those in Fig. 2a. Direction of the marks was arbitrary and signified that the crack growth was also arbitrary along the center line through the open hole.

Meanwhile, with breakage of fibers around the open hole, the load was transferred to the neighboring fibers through the fiber/matrix interface, leaving shear marks both in the OHT and OHC samples. These marks can be seen in Fig. 3. However, it was noticed that they were much less in the OHT samples than in the OHC ones. This indicated that the failure of OHT samples was dominated by the failure of carbon fibers, while in the OHC ones, it was dominated by the failure of both carbon fibers and matrix.

Some of the shear marks originating during the load transfer among carbon fibers in the OHT and OHC samples are presented in Fig. 3. They emerged due to the mismatch between the elastic moduli and strains of carbon fibers and resin. These

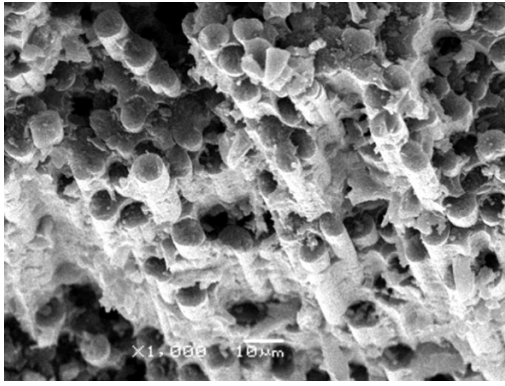


Fig. 4. Fiber pull-outs in an OHT sample.

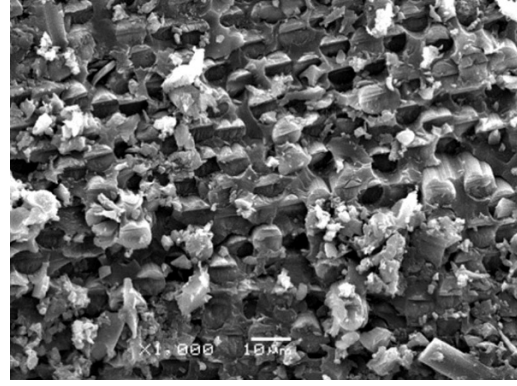


Fig. 5. Microbuckling and crushing of carbon fibers in an OHC sample.

marks indicated that the load had been transferred from one layer to another through shearing at the fiber/matrix interface both in the OHT and OHC samples, but their quantity differed. The greater quantity of shear marks in OHC samples pointed to a higher load transfer and higher shear in the OHC samples than in the OHT ones.

It was also observed that fiber surfaces in both the types of samples were fairly intact, undamaged, and without any sign of macro- or microcracks. As the tensile load increased, fibers were pulled out of the matrix of the OHT samples, but an increasing compressive load led their microbuckling and crushing in the OHC samples. The fiber pull-out and microbuckling/crushing occurred close to the open-hole area.

Significant fiber pull-outs can be observed in the micrograph of an OHT sample shown in Fig. 4. As seen, the carbon fibers are distributed evenly, but the shape, size, and contrast of their cross-sectional images vary over the surface. Some of them are bright and big, signifying that their location was more close to the SEM electron beam, whereas others are dark and small due to their greater distance from the beam. This suggests that fibers broke at different locations (relatively far) due to the pronounced crack bridging and crack deflection mechanisms.

The microbuckled and crushed fibers present in an OHC sample are shown in Fig. 5. As seen, the distribution of carbon fibers in the resin is homogenous, with a similar shape, size, and contrast of their cross-sectional images over the fracture surface. This indicates that the breakage of fibers occurred close to each other, with less pronounced crack bridging and crack deflection mechanisms than in the OHT samples. Significant key features were also observed on a deep and careful examination of the cross-sectional images of carbon fibers (at a higher magnification) in the OHT and OHC samples. These features were different from each other and gave information about the loading conditions of samples which caused their failure, i.e., tensile or compressive. Such information would be of great value in structural failure analyses.

The cross-sectional view of carbon fibers after an OHT test is shown in Fig. 6. The radial patterns of fibers — the key feature of pure tensile fracture of carbon fibers — are seen. These patterns are clearly distinguished on the cross section of individual fibers. They were found in groups and probably had originated at the circumference of fibers under the influence of a combination action of residual stresses in the matrix and the additional stresses arising in the fracture process.

A cross-sectional view of carbon fibers after an OHC test is shown in Fig. 7. A shear crippling due to the microbuckling of fibers caused by the compressive load is observed. The crippling produced the key feature of fracture known as chop marks. Three specific regions of chop marks on fiber ends can also be seen in the Fig. 7. The first is the tensile region, indicated by fiber radials, the second is the compression region, indicated by a flat, often angled, fracture surface, and the third is the neutral axis or line separating the two regions. After reaching the ultimate stress/strength, the OHT and OHC samples both failed spontaneously (in the hole area) without any plastic deformation. The final fracture surfaces and crack paths for the OHT and OHC samples were significantly different.

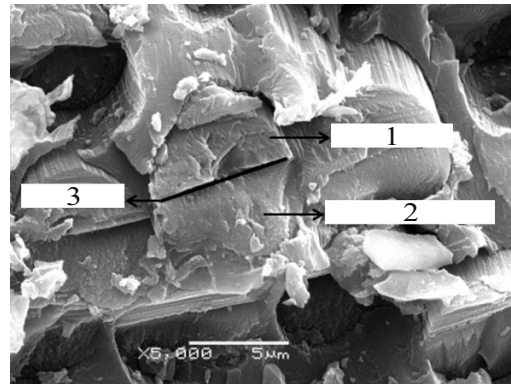
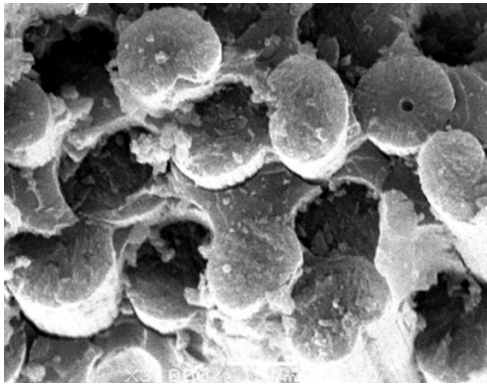


Fig. 6. Radial patterns on the cross section of carbon fibers under tensile loading.

Fig. 7. Chop marks on the cross section of carbon fibers under compressive loading: 1 — tensile region, 2 — compressive region, and 3 — neutral axis .

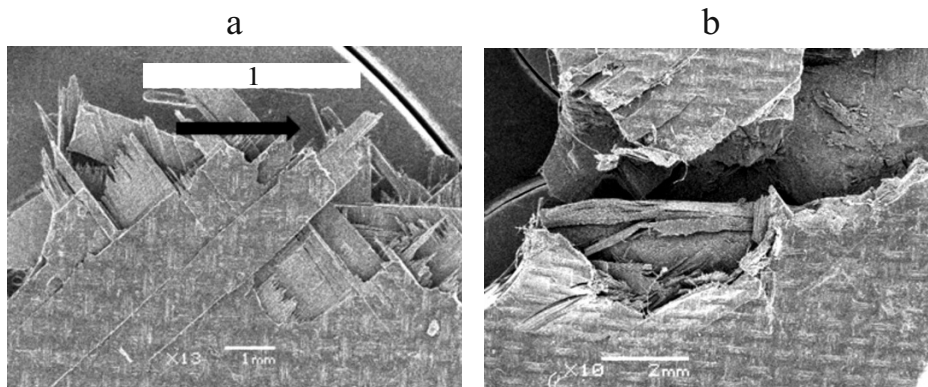


Fig. 8. Photomicrographs of the final fracture and crack path (1) in OHT (a) and OHC (b) samples..

Figure 8 presents a photomicrograph of the final fracture and the crack path for an OHT sample, which was neither smooth (straight) nor heavily splintered. Fibers were broken randomly in an irregular path with cracks deflected along the fiber direction, but only over short distances, pointing to a fairly good interfacial bond between the carbon fibers and epoxy matrix. Some fiber splintering was also noticed.

The final fracture and crack path for an OHC sample is shown in Fig. 8b. The crack paths in the OHC samples were straighter and less jagged than in the OHT ones. Fibers were broken randomly in the form of groups in an irregular path, which was much shorter than that in the OHT samples. Microbucklings due to compression, with almost no individual fiber splinterings, could also be seen.

3.3. Failure mechanisms

Despite the soft and smooth drilling, microcracks were generated at the periphery of holes (Fig. 1), which acted as stress concentration points. Moreover, the region close to an open hole also became lean and weak due to the removal of the composite material. Hence, upon application of a tensile load to an open-hole composite sample, the microcracks at the inner rim of the hole coalesced and formed a macrocrack, which started its propagation and left river pattern marks on the resin adhered to fibers (Fig. 2), showing the direction of crack growth from the center to the edge of sample (perpendicular to the

applied load). Meanwhile, some part of the load was also transferred to other carbon fiber plies through interlaminar shearing, with the appearance of hackles (shear marks, Fig. 3) in the matrix phase. As the tensile load increased, the fibers in the weak region close to the open hole broke and were pulled out of the matrix (Fig. 4), revealing radial fiber patterns on fiber cross sections (Fig. 6). After reaching the ultimate stress, the samples failed suddenly, exhibiting irregular crack paths with detectable deflections of cracks.

As the OHT and OHC samples had an open hole at their center, the microdamage in them initiated from the hole boundary upon application of a compressive load. The damage grew along the center line of the open-hole in a random direction perpendicular to the applied load, leaving river pattern marks (Fig. 2b), but the direction of this pattern in the OHC samples was significantly different from that in the OHT (Fig. 2a). The load transfer among layers was very similar to that in the OHT samples, but with much more shear hackle marks (Fig. 3b). As in the OHT samples, with increase in load, the carbon fibers broke across the entire width of samples in the same region, but by microbuckling and crushing (Fig. 5), exposing chop marks (Fig. 7) in spite of fiber radials in the OHT samples. The ultimate failure occurred with a crack passing through the hole in an uneven crack path (Fig. 8a) and with a smaller crack deflection than in the OHT samples.

Conclusions

OHT and OHC tests were performed on single-open-hole carbon-fiber-reinforced composite samples to get fracture surfaces to be explored by the SEM. A comparison of SEM micrographs of the OHT and OHC samples highlighted valuable information and key differences. Both in the OHT and OHC samples, the fracture initiated by the coalescence of microcracks at the periphery of the drilled hole and grew along the center line containing the hole. The load transfer among fibers occurred through shearing leaving shear marks in both the types of samples, which were found less in the OHT and more in the OHC samples. The failure of the OHT samples was dominated by fiber pull-outs and fiber breakage. The failure of the OHC sample was dominated by the damage of both fibers and resin with features of microbuckling and shear crippling. The key characteristic features of fiber radials and chop marks were found at the fiber ends of the OHT and OHC samples, respectively. The final failure surface of the OHT samples exhibited a significant fiber splintering, crack deflection, and crack bridging. The final failure surface of the OHC samples was more even and less jagged, with almost no fiber splinterings.

Acknowledgement. This work was supported by NUAA Fundamental Research Funds (NO.NS2015060) and the Jiangsu collaborative innovation center for advanced inorganic functional composites.

REFERENCES

1. J. Backlund and C. G. Aronsson, "Tensile fracture of laminates with holes," *J. Compos. Mater.*, 20259-85 (1986).
2. I. Eriksson and C. G. Aronsson, "Strength of tensile loaded graphite/epoxy laminates containing cracks, open and drilled holes," *J. Compos. Mater.*, 24456-24482 (1990).
3. S. C. Tan and R. Y. Kim, "Damage accumulation and fracture of notched composite laminates under tensile and compressive loading," In: *Composite Materials: Testing and Design ASTM STP 1120*, (1992).
4. A. B. Morais, A. T. Marques, and P. T. Castro, "Open-hole tension and compression strengths of carbon/epoxy quasi-isotropic laminates," *Proc. 8th Europ. Conf. on Composite Materials (ECCM8)*. Naples: (1998).
5. K. Chang, S. Liu, and F. Chang, "Damage tolerance of laminated composites containing an open hole and subjected to tensile loadings," *J. Compos. Mater.*, 25274-25301. (1991).
6. S. R. Hallett and M. R. Wisnom, "Experimental investigation of progressive damage and the effect of layup in notched tensile tests," *J. Compos. Mater.*, 40119-40141 (2006).
7. J. Lee and C. Soutis, "Thickness effect on the compressive strength of T800/924C carbon fibre-epoxy laminates," *Composites: Part A*, **36** (2005).

8. Y. K. Boey and Y. W. Kwon, "Progressive damage and failure strength of notched woven fabric composites under axial loading with varying strain rates," *Compos. Struct.*, **96**, No. 0, 824-832 (2013).
9. Y. Zheng, X. Q. Cheng, and B. Yasir, "Effect of stitching on plain and open-hole strength of CFRP laminates," *Chinese J. of Aeronautics*, **25** (2012).
10. S. Y. Kim, J. M. Koo, D. D.-W. Kim, and C. S. Seok, "Prediction of the static fracture strength of hole notched plain weave CFRP composites," *Compos. Sci. and Technol.*, **71** (2011).
11. M. R. Wisnom and S. R. Hallett, "The role of delamination in strength, failure mechanism and hole size effect in open hole tensile tests on quasi-isotropic laminates," *Composites: Part A*, **40** (2009).
12. A. J. M. Jasso, J. E. Goodsell, A. J. Ritchey, R. B. Pipes, and M. Koslowski, "A parametric study of fiber volume fraction distribution on the failure initiation location in open hole off-axis tensile specimen," *Compos. Sci. and Technol.*, **71** (2011).
13. H. Suemasu, H. Takahashi, and T. Ishikawa, "On failure mechanisms of composite laminates with an open hole subjected to compressive load," *Compos. Sci. and Technol.*, **66** (2006).
14. T. Flatscher, M. Wolfahrt, G. Pinter, and H. E. Pettermann, "Simulations and experiments of open hole tension tests – Assessment of intra-ply plasticity, damage, and localization," *Compos. Sci. and Technol.*, **72**, 1090–1095 (2012).
15. P. P. Camanho, G. H. Erçin, G. Catalanotti, S. Mahdi, and P. Linde, "A finite fracture mechanics model for the prediction of the open-hole strength of composite laminates," *Composites: Part A*, **43** (2012).
16. E. Abisset, F. Daghia, and P. Ladevèze, "On the validation of a damage mesomodel for laminated composites by means of open-hole tensile tests on quasi-isotropic laminates," *Composites: Part A* **42** (2011).
17. J. Wang, P. J. Callus, and M. K. Bannister, "Experimental and numerical investigation of the tension and compression strength of un-notched and notched quasi-isotropic laminates," *Compos. Struct.*, **64** (2004).
18. P. P. Camanho, P. Maimí, and C. G. Dávila, "Prediction of size effects in notched laminates using continuum damage mechanics," *Compos. Sci. and Technol.*, **67**, No. 13, 2715-2727 (2007).
19. F. Pierron, B. Green, M. R. Wisnom, and S. R. Hallett, "Full-field assessment of the damage process of laminated composite open-hole tensile specimens. Part II: Experimental results," *Composites: Part A*, **38** (2007).
20. F. Pierron, B. Green, and M. R. Wisnom, "Full-field assessment of the damage process of laminated composite open-hole tensile specimens. Part I: Methodology," *Composites: Part A*, **38**, 2307–2320 (2007).
21. L. Farge, J. Varna, and Z. Ayadi, "Damage characterization of a cross-ply carbon fiber/epoxy laminate by an optical measurement of the displacement field," *Compos. Sci. and Technol.*, 7094–7101 (2010).
22. A. Yudhanto, N. Watanabe, Y. Iwahori, and H. Hoshi, "Effect of stitch density on tensile properties and damage mechanisms of stitched carbon/epoxy composites," *Composites: Part B; Engineering*, (2012).
23. A. Yudhanto, N. Watanabe, Y. Iwahori, and H. Hoshi, "The effects of stitch orientation on the tensile and open hole tension properties of carbon/epoxy plain weave laminates," *Materials and Design*, 35563–35571 (2012).
24. A. Yudhanto, N. Watanabe, Y. Iwahori, and H. Hoshi, "Open hole fatigue characteristics and damage growth of stitched plain weave carbon/epoxy laminates," *Int. J. of Fatigue*, **43** (2012).
25. R. M. O'Higgins, M. A. McCarthy, and C. T. McCarthy, "Comparison of open hole tension characteristics of high strength glass and carbon fibre-reinforced composite materials," *Compos. Sci. and Technol.*, **68** (2008).
26. ASTM Standard D5766/D5766M – 02, Standard test method for open hole tensile strength of polymer matrix composite laminates 2002: American Society for Testing and Materials.
27. ASTM Standard D6484/D6484M – 04, Standard test method for open-hole compressive strength of polymer matrix composite laminates. 2004: American Society for Testing and Materials.